Analysis of CDMA Signal Spectral Regrowth and Waveform Quality

Vladimir Aparin

***Abstract*—Closed-form expressions for the spectral regrowth and waveform quality of a reverse-link code divison multiple access (CDMA) signal passed through a weakly nonlinear circuit are derived using the power series and statistical methods. The third-order nonlinearity is expressed in terms of IP_3 to include the memory effects of the circuit in-band and out-of-band reactances. The analysis is based on a time-domain model of the signal that gives more accurate distortion estimates than the widely used Gaussian approximation. The model is used to derive the probability density function and other statistical properties of the CDMA signal to compare them to the Gaussian noise properties. Differences in statistics and distortions of OQPSK and QPSK modulated signals are discussed.**

***Index Terms*—Autocorrelation, CDMA, distortion, distribution functions, nonlinear circuits, power spectra, statistics.**

I. Introduction

DUE TO the time-varying envelope of a code divison multiple access (CDMA) signal, its distortion has a significant consideration in IS-95 transmitters. Intermodulation by the transmitter odd-order nonlinearities widens the CDMA signal spectrum. This widening is called *spectral regrowth* and is characterized by the adjacent channel power ratio (ACPR). The spectral regrowth power in the adjacent channel acts as an interference to other users in the cell using this channel. The intermodulation distortion (IMD) also contaminates the transmitted channel itself, degrading its signal-to-noise ratio (SNR). The latter is typically measured as a waveform quality factor or error vector magnitude.

Predicting distortion of a CDMA signal has always been challenging due to its pseudorandom nature. Several circuit simulation and behavioral modeling techniques have been proposed [1]. The circuit simulation techniques work in the time domain (transient analysis), frequency domain (harmonic balance, Volterra series), or both domains (envelope analysis). The transient analysis is impractical for handling CDMA signals because its simulation interval must be at least as long as the data-spreading PN code period while the time step is limited by the RF carrier. It also requires the fast Fourier transform (FFT) to convert the computed waveform to the frequency domain—another time-consuming step.

The harmonic balance (HB) represents a response as a Fourier series with time-invariant coefficients. It is only efficient for periodic and quasi-periodic responses that can be described by a few tones. The number of tones for a digitally modulated carrier is set by the number of its envelope samples and typically ranges from several hundred to several thousand [2], making the computation time and memory-intensive. The phases of the tones should be equal to the phases of the envelope samples to correctly model the signal statistics. The Volterra analysis described in [3] also uses a multitone model of a narrow-band signal, but it only needs k or fewer tones to compute the kth-order transfer function. This transfer function has to be computed for all possible linear combinations of the input tones, making the analysis inefficient unless the order of the dominating nonlinearity is limited to $k = 3$ and the transfer functions for the tones with the same spacing are assumed to be equal.

The envelope analysis [4], [5] uses time-variant phasors to represent a solution. This drastically reduces their number for a nonperiodic response. An input CDMA signal is modeled by just one tone (carrier) with a time-varying complex envelope. The memory effects of the circuit reactances on the envelope are computed by a time-domain integration of the circuit equations for just the envelope. The integration time step is set by the envelope bandwidth rather than the carrier frequency. At each time point, the circuit is modified to include the transient solution and analyzed using a single-tone HB to obtain the instantaneous envelopes of the carrier and its harmonics at each node. Despite so many HB runs, the envelope method is faster than the transient method, but requires more memory [4].

The behavioral modeling techniques were developed to speed up the spectral regrowth analysis. They differ by the circuit model (single- or two-tone transfer function) and by the signal representation (envelope samples, statistics or discrete spectrum). The technique described in [6] can be viewed as a simplified version of the envelope analysis. It skips the time-domain integration, assuming that the circuit memory for the envelope is negligible. For each input envelope sample, the carrier output amplitude and phase are found from the precomputed single-tone AM–AM and AM–PM characteristics of the circuit using interpolation. The technique described in [7] predicts the output envelope spectrum analytically with statistical methods applied to a CDMA signal processed by a complex power series fitted to the AM–AM and AM–PM characteristics of the circuit. For simplicity, the signal statistics are assumed to be the same as those of a narrow-band Gaussian noise (NBGN). The author of [8] also uses the power series and statistical methods, but, recognizing that a QPSK signal does not behave as NBGN, computes its higher order moments numerically. All three techniques are based on the single-tone

Manuscript received March 30,2001; revised August 21, 2001.

The author is with QUALCOMM Inc., San Diego, CA 92121 USA (e-mail: vaparin@qualcomm.com).

Publisher Item Identifier S 0018-9480(01)10464-3.

transfer functions and, therefore, do not take into account the baseband and second harmonicimpedances of the circuit. These impedances can significantly affect the third-order distortion [9].

The technique described in [10] is based on the two-tone transfer function. It expresses the circuit third-order nonlinearity in terms of the third-order intermodulation product (IP_3) that includes the effect of the out-of-band impedances. As in [7], the CDMA signal is modeled as NBGN and its statistics are transformed by a power series. In [11], the spectral regrowth is expressed in terms of the two-tone IMD as well, but the analysis is performed in the frequency domain by modeling a CDMA signal as n tones of equal power and random phases uniformly spaced within the signal bandwidth. With n approaching infinity, this multitone excitation becomes NBGN.

The Gaussian approximation is acceptable only for a forward-link CDMA signal with a large number of Walsh-coded channels transmitted at the same frequency. These channels are summed analogically before QPSK modulation and the resulting baseband signal approaches a normal distribution with an increasing number of the channels according to the central limit theorem. The signal statistics for a lightly loaded forward link depend on the number of channels and their codes [12], [13]. A signal transmitted by a mobile station carries only one channel at a time and does not behave as NBGN.[1] In [14], the authors showed that the Gaussian approximation of the reverse-link CDMA signal leads to inaccurate estimates of the cross-modulation distortion in mobile receivers and proposed a more accurate model of the signal based on its description in the time domain.

This model is used here to derive the probability density function (PDF) and other statistical properties of a reverse-link CDMA signal and compare them to those of NBGN. Differences in statistics and distortions of OQPSK and QPSK modulated signals are discussed. The spectral regrowth and waveform quality of a CDMA signal passed through a weakly nonlinear circuit are analyzed using the power series and statistical methods. The memory effects of the circuit in- and out-of-band reactances are included by expressing the third-order nonlinearity through IP_3. The analytical results are compared to the measured data.

II. Time-Domain Model of the CDMA Signal

The time-domain model of a CDMA signal proposed in [14] is derived according to a simplified IS-95 reverse-link modulation scheme shown in Fig. 1. The Walsh-coded data is first split into the I and Q channels and spread by the orthogonal PN codes at the rate B of 1.2288 Mc/s. The Q channel is delayed by 1/2 chip, resulting in OQPSK spreading (T in Fig. 1 is the chip time equal to $1/B$). The spreading codes are assumed to be infinitely long and each chip is approximated with the Dirac

[1]A signal received by a base station contains transmissions from several users and multipaths. For a large number of users occupying the same frequency, this signal can be approximated by NBGN, but its distortion in the base station receiver is typically no concern.

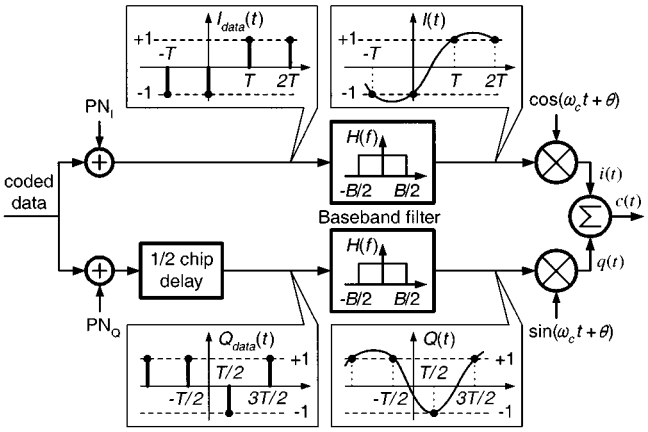

Fig. 1. Simplified model of IS-95 CDMA reverse-link modulator.

delta function $\delta(t)$. Thus, the spread I and Q data streams can be modeled as

$$I_{\text{data}}(t) = \sum_{k=-\infty}^{\infty} i_k \delta(Bt + \phi/\pi - k)$$

$$Q_{\text{data}}(t) = \sum_{k=-\infty}^{\infty} q_k \delta(Bt + \phi/\pi - k + 1/2)$$

where ϕ is a random phase uniformly distributed in $(0,\ \pi)$ and i_k and q_k are independent random numbers taking values of ± 1 with equal probability. These binary numbers are the results of the modulo-2 addition of the data bits with the spreading code chips. Due to the PN code randomness, various numbers within the same spread-data stream are also considered to be independent.

With an acceptable accuracy, the IS-95 baseband pulse-shaping filter can be modeled as an ideal low-pass filter with the cutoff frequency $B/2$ and impulse response $h(t) = B\,\text{sinc}(Bt)$, where $\text{sinc}(z) = \sin(\pi z)/(\pi z)$. The I and Q spread-data signals passed through the filter become

$$I(t) = \sum_{k=-\infty}^{\infty} i_k \,\text{sinc}(Bt + \phi/\pi - k)$$

$$Q(t) = \sum_{k=-\infty}^{\infty} q_k \,\text{sinc}(Bt + \phi/\pi - k + 1/2).$$

The filtered I and Q signals are modulated on two carriers in quadrature and summed, producing the transmitted signal

$$c(t) = i(t) + q(t) \tag{1}$$

where $i(t) = I(t)\cos(\omega_c t + \theta)$, $q(t) = Q(t)\sin(\omega_c t + \theta)$, ω_c is the angular frequency of the carriers, and θ is their random phase independent of ϕ and uniformly distributed in $(0,\ 2\pi)$. Equation (1) is the time-domain model of a reverse-link CDMA signal with unity variance. In general, this signal can be described as $\sqrt{V_c}c(t)$ where V_c^2 is its mean-square voltage (or variance). A forward-link CDMA signal is QPSK modulated and, for a single active Walsh-coded channel, is also modeled by (1) without 1/2 in the sinc-function argument of $Q(t)$.

According to the interpolation formula of the sampling theorem [15], any signal confined to the band $(-B/2, B/2)$ can be accurately represented by an infinite sum of the sinc pulses spaced periodically $1/B$ s apart and weighted by the signal samples at the corresponding time instants. Thus, (1) can be viewed as a general time-domain model of two band-limited signals OQPSK-modulated on a carrier with i_k and q_k being their samples. If these samples are normally distributed, (1) describes a narrow-band Gaussian noise. Thus, the important difference between the models of the CDMA signal and NBGN is in the statistical properties of the i_k and q_k samples.

III. Statistical Properties of the CDMA Signal and NBGN

The correlation properties of i_k and q_k for the CDMA signal $c(t)$ and NBGN $n(t)$ are the same and given by

$$E\{i_k q_l\} = E\{i_k\}E\{q_l\} = 0$$
$$E\{i_k i_l\} = E\{q_k q_l\} = \begin{cases} 1, & \text{if } k = l \\ 0, & \text{if } k \neq l \end{cases}$$

where $E\{\,\}$ is the statistical average (or expectation). Distortion analysis also requires the knowledge of the nth moments of the i_k and q_k samples. For the CDMA signal,

$$E\{i_k^n\} = E\{q_k^n\} = \begin{cases} 0, & \text{if } n \text{ is odd} \\ 1, & \text{if } n \text{ is even} \end{cases}$$

and, for NBGN [16],

$$E\{i_k^n\} = E\{q_k^n\} = \begin{cases} 0, & \text{if } n \text{ is odd} \\ 1 \cdot 3 \cdot 5 \cdots (n-1), & \text{if } n \text{ is even.} \end{cases}$$

Thus, the higher even-order moments of the envelope I and Q samples for NBGN exceed those for the CDMA signal which causes NBGN to exhibit a stronger distortion.

Since $E\{i_k\} = E\{q_k\} = 0$, both the CDMA signal and NBGN have *zero mean*. Due to the randomness and zero cross correlation of ϕ and θ, the statistical properties of $i(t)$ and $q(t)$ are time-independent. Thus, the CDMA signal and NBGN and their distortions are *stationary* processes under the made assumptions. To shorten the formulas, the time variable t will be set to zero in further derivations without losing accuracy. As shown in Appendix A, $c(t)$ and $n(t)$ have the same autocorrelation function given by

$$R_c(\tau) = R_n(\tau) = \text{sinc}(B\tau)\cos(\omega_c \tau).$$

The Fourier transform of this autocorrelation function yields the following two-sided power spectral density (PSD) function for both $c(t)$ and $n(t)$:

$$S_c(\Omega) = S_n(\Omega) = \begin{cases} 1/(2B), & |\Omega| \leq 1 \\ 0, & \text{otherwise} \end{cases}$$

where $\Omega = 2(|f| - f_c)/B$ is the normalized frequency offset and $f_c = \omega_c/(2\pi)$. In the rest of the paper, to shorten expressions for PSD, only the frequency ranges where it is nonzero will be mentioned presuming that PSD is zero elsewhere.

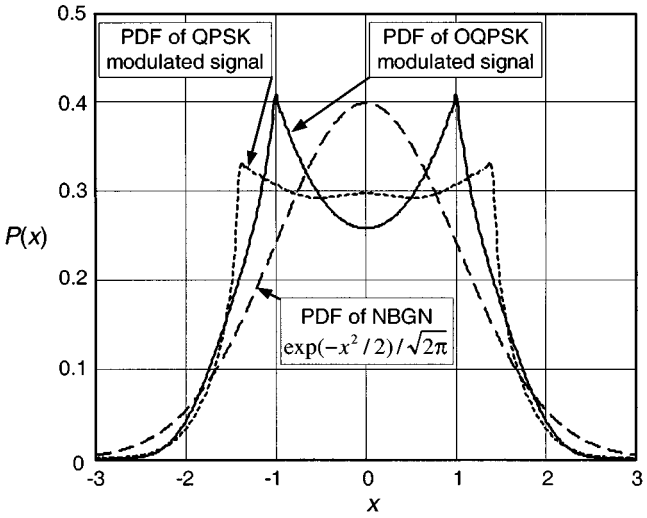

Fig. 2. PDFs of OQPSK and QPSK modulated signals compared to a Gaussian PDF.

The characteristic function of the CDMA signal is derived in Appendix B and is given by

$$M(v) = \frac{1}{2\pi^2}\int_0^{2\pi} d\theta \int_0^{\pi} d\phi \prod_{k=-\infty}^{\infty} \cos\left[v\cos(\theta)\frac{\sin(\phi)}{\phi - k\pi}\right] \cdot \cos\left[v\sin(\theta)\frac{\cos(\phi)}{\phi - k\pi + \pi/2}\right].$$

The above integral belongs to a group of sinc-related integrals that do not have analytical solutions according to [17]. It was computed numerically and then, using the inverse Fourier transform, converted to a PDF that is plotted as a solid line in Fig. 2 where x is the instantaneous voltage and $P(x)$ is its probability. The characteristic function of a QPSK modulated signal such as a single-channel forward-link CDMA signal is the same as the above $M(v)$ with $\pi/2$ omitted and $\cos(\phi)$ replaced with $\sin(\phi)$ in the second brackets. Its PDF obtained by the inverse FFT is also plotted in Fig. 2 together with the PDF of NBGN for comparison. As can be seen, PDFs of OQPSK and QPSK modulated signals significantly differ from the Gaussian PDF and, therefore, the expansion formulas of the higher order joint normal moments used in [7] and [10] cannot be used in calculating distortions of these signals. To the author's knowledge, the joint moments of a CDMA signal have not yet been derived in closed form and published.

IV. Joint Moments of the CDMA Signal

Distortion is generated by the nonlinearities of the circuit transfer function that is usually expanded into a power series around the operating point as

$$y(t) = \sum_{n=1}^{\infty} y_n(t) \quad \text{with,} \qquad y_n(t) = a_n x^n(t) \tag{2}$$

where $y(t)$ is the output signal, $x(t)$ is the input signal, and a_ns are the expansion coefficients. a_1 is the linear gain of the circuit and higher order coefficients characterize the strength of

the corresponding nonlinearities. If $x(t)$ is stationary, the autocorrelation of the output is given by

$$R_y(\tau) = E\Big\{y(0)y(\tau)\Big\} = \sum_{m=1}^{\infty}\sum_{n=1}^{\infty} a_m a_n R_x(\tau; m, n)$$

where $R_x(\tau; m, n) = E\{x^m(0)x^n(\tau)\}$ is the $(m+n)$th-order joint moment of the input signal. Its expansion for a normally distributed zero-mean input signal is given in [18].

Let $R_c(\tau; m, n)$ denote the joint moment of the CDMA signal $c(t)$, i.e., $E\{c^m(0)c^n(\tau)\}$. Using (1), we obtain

$$\begin{aligned} R_c(\tau; m, n) &= E\Big\{[i+q]^m[i_\tau + q_\tau]^n\Big\} \\ &= E\left\{\sum_{k=0}^{m}\binom{m}{k} i^k q^{m-k} \sum_{l=0}^{n}\binom{n}{l} i_\tau^l q_\tau^{n-l}\right\} \\ &= \sum_{k=0}^{m}\sum_{l=0}^{n}\binom{m}{k}\binom{n}{l} \\ &\quad \cdot E_\theta\Big\{\cos^k(\theta)\cos^l(\omega_c\tau+\theta) \\ &\qquad \cdot \sin^{m-k}(\theta)\sin^{n-l}(\omega_c\tau+\theta)\Big\} \\ &\quad \cdot E_\phi\Big\{E_i\{I^k I_\tau^l\}E_q\{Q^{m-k}Q_\tau^{n-l}\}\Big\} \end{aligned}$$

where i, q, i_τ, and q_τ denote $i(0)$, $q(0)$, $i(\tau)$, and $q(\tau)$, respectively, and I, Q, I_τ, and Q_τ denote $I(0)$, $Q(0)$, $I(\tau)$, and $Q(\tau)$, respectively. The averages over i_k and q_k samples, $E_i\{I^k I_\tau^l\}$ and $E_q\{Q^{m-k}Q_\tau^{n-l}\}$, are the joint moments of $I(t)$ and $Q(t)$, respectively. They can be treated in the same way as the moments of a random binary pulse train [19].

Let g_i denote $\mathrm{sinc}(\phi/\pi - k)$, h_i denote $\mathrm{sinc}(B\tau + \phi/\pi - k)$, g_q denote $\mathrm{sinc}(\phi/\pi - k + 1/2)$, h_q denote $\mathrm{sinc}(B\tau + \phi/\pi - k + 1/2)$, and parentheses denote the summation over k, i.e.,

$$(g_i^m) = \sum_{k=-\infty}^{\infty} \mathrm{sinc}^m(\phi/\pi - k)$$

and

$$(g_i^m h_i^n) = \sum_{k=-\infty}^{\infty} \mathrm{sinc}^m(\phi/\pi - k)\mathrm{sinc}^n(B\tau + \phi/\pi - k). \quad (3)$$

The moments of $I(t)$ and $Q(t)$ can then be expanded in terms of the sums similar to (3). Only the even-order moments will be nonzero. Their expansions needed to compute the distortion from the third or lower order nonlinearity ($k \le 3, l \le 3$) are shown in Table I. The closed-form results of the individual sums are obtained with a symbolic math and are given in Table II. These results are applicable to OQPSK and QPSK modulated signals and, therefore, both signals should exhibit the same spectral regrowth if the third-order nonlinearity is dominant. However, the $I(t)$ and $Q(t)$ moments generated by the fifth or higher order nonlinearity are different for the two signals resulting in their different spectral regrowth under strong signal conditions.

TABLE I
MOMENTS OF $I(t)$ AND $Q(t)$

k,l	$E_i\{I^k I_\tau^l\}, E_q\{Q^k Q_\tau^l\}$
1,1	$(gh)^a$
2,0	(g^2)
0,2	(h^2)
2,2	$-2(g^2h^2) + 2(gh)^2 + (g^2)(h^2)$
3,1	$-2(g^3h) + 3(g^2)(gh)$
1,3	$-2(gh^3) + 3(h^2)(gh)$
3,3	$16(g^3h^3) - 6(h^2)(g^3h) - 6(g^2)(gh^3)$ $-18(gh)(g^2h^2) + 9(g^2)(h^2)(gh) + 6(gh)^3$

[a] g and h denote g_i and h_i respectively in the $E_i\{I^k I_\tau^l\}$ expansions and g_q and h_q respectively in the $E_q\{Q^k Q_\tau^l\}$ expansions.

TABLE II
CLOSED-FORM EXPRESSIONS FOR $(g^m h^n)$ SUMS

Sum	Result
(gh)	$\mathrm{sinc}(B\tau)$
(g^2), (h^2)	1
$E_\phi\{(g^2h^2)\}$	$\dfrac{1-\mathrm{sinc}(2B\tau)}{(\pi B\tau)^2}$
$E_\phi\{(g^3h)\}$, $E_\phi\{(gh^3)\}$	$\dfrac{\mathrm{sinc}(B\tau)}{2} + \dfrac{\mathrm{sinc}(B\tau) - \cos(\pi B\tau)}{2(\pi B\tau)^2}$
$E_\phi\{(g^3h^3)\}$	$3/4\{\mathrm{sinc}(B\tau)[3/2 + (\pi B\tau)^2]$ $+3/2\ \mathrm{sinc}(3B\tau) - 3\cos(\pi B\tau)\}/(\pi B\tau)^4$

V. ANALYSIS OF CDMA SIGNAL DISTORTION

Let the output signal of a nonlinear circuit be expanded in the power series (2) where $x(t) = \overline{V_c}c(t)$ and $c(t)$ is given by (1). Terms of the order higher than three will be neglected here, i.e., the circuit is assumed *weakly nonlinear*. The second-order term $y_2(t)$ will be omitted as well since it does not contribute to the in-band distortion. The autocorrelation function of the output is then

$$\begin{aligned} R_y(\tau) &= E\Big\{[y_1(0) + y_3(0)][y_1(\tau) + y_3(\tau)]\Big\} \\ &= E\Big\{y_1(0)y_1(\tau)\Big\} + E\Big\{y_1(0)y_3(\tau)\Big\} \\ &\quad + E\Big\{y_3(0)y_1(\tau)\Big\} + E\Big\{y_3(0)y_3(\tau)\Big\}. \end{aligned} \quad (4)$$

The first summand in (4) is the autocorrelation of the linear response of the circuit $y_1(t)$. The second and third summands are the cross correlations describing the in-channel portion of the third-order response $y_3(t)$ correlated to $y_1(t)$ and responsible for the gain compression or expansion. The last summand is the autocorrelation of $y_3(t)$ that gives the spectral regrowth.

A. Linear Response

The autocorrelation function of the linear response is

$$\begin{aligned} E\Big\{y_1(0)y_1(\tau)\Big\} &= a_1^2\overline{V_c^2}E\Big\{c(0)c(\tau)\Big\} \\ &= P_o\mathrm{sinc}(B\tau)\cos(\omega_c\tau) \end{aligned}$$

where $P_o = a_1^2\overline{V_c^2}$ is the total output power of the linear response. The Fourier transform of the above expression gives the following PSD:

$$S_{\text{lin}}(\Omega) = P_o/(2B), \qquad \text{for } |\Omega| \le 1.$$

The derived PSD is easier to use if it is converted to the power in a frequency band Δf much narrower than the CDMA signal bandwidth B. Δf corresponds to the resolution bandwidth of a spectrum analyzer that is typically selected to be 30 kHz for ACPR measurements. Integrating $S_{\text{lin}}(\Omega)$ over Δf and taking into account the negative frequency spectrum (adds factor of 2) results in

$$P_{\text{lin}}(\Omega) = P_o\Delta f/B, \qquad \text{for } |\Omega| \le 1.$$

B. Distortion Causing Gain Compression or Expansion

The second summand in (4) can be evaluated as follows:

$$\begin{aligned} R_{y_1y_3}(\tau) &= E\Big\{y_1(0)y_3(\tau)\Big\} = a_1a_3\overline{V_c^4}E\Big\{(i+q)(i_\tau+q_\tau)^3\Big\} \\ &= a_1a_3\overline{V_c^4}E\Big\{ii_\tau^3+qq_\tau^3+3ii_\tau q_\tau^2+3i_\tau^2qq_\tau\Big\} \end{aligned}$$

where the products iq_τ^3, i_τ^3q, $3ii_\tau^2q_\tau$, and $3i_\tau qq_\tau^2$ are omitted because their averages are zero. Replacing i, i_τ, q, and q_τ with the corresponding $i(0)$, $i(\tau)$, $q(0)$, and $q(\tau)$ definitions from (1) and taking the average over θ, we obtain

$$\begin{aligned} R_{y_1y_3}(\tau) = \frac{3a_1a_3\overline{V_c^4}}{8}\cos(\omega_c\tau)\int_0^\pi\frac{d\phi}{\pi} \\ \cdot[E_i\{II_\tau^3\}+E_q\{QQ_\tau^3\}+E_i\{II_\tau\}E_q\{Q_\tau^2\} \\ +E_i\{I_\tau^2\}E_q\{QQ_\tau\}]. \end{aligned}$$

Using the results from Tables I and II, we obtain

$$\begin{aligned} R_{y_1y_3}(\tau) = \frac{3a_1a_3\overline{V_c^4}}{4}\cos(\omega_c\tau) \\ \cdot\left[3\,\text{sinc}(B\tau)-\frac{\text{sinc}(B\tau)-\cos(\pi B\tau)}{(\pi B\tau)^2}\right]. \end{aligned}$$

The third summand in (4) is equal to the second one. The Fourier transform of $2R_{y_1y_3}(\tau)$ gives the following PSD of the in-channel distortion:

$$S_{\text{ICD}}(\Omega) = 3a_1a_3\overline{V_c^4}(\Omega^2+5)/(8B), \qquad \text{for } |\Omega| \le 1. \quad (5)$$

If the sign of a_3 is opposite to that of a_1, S_{ICD} is subtracted from S_{lin} causing the gain compression. If the signs are the same, S_{ICD} is added to S_{lin} resulting in the gain expansion. In the following analysis, the gain compression is assumed.

The third-order expansion coefficient a_3 can be expressed as a function of the output third-order intercept point OIP_3 as

$$a_3 = -2a_1^3/(3\cdot OIP_3).$$

Substituting a_3 into (5) and converting the PSD into the power in Δf, we get

$$P_{\text{ICD}}(\Omega) \approx -P_o^2\Delta f(\Omega^2+5)/(2B\cdot OIP_3) \qquad \text{for } |\Omega| \le 1$$

where "$\approx$" is used because, instead of integrating $S_{\text{ICD}}(\Omega)$ over $(-f-\Delta f,\ -f)$ and $(f,\ f+\Delta f)$, it was multiplied by $2\Delta f$ to obtain $P_{\text{ICD}}(\Omega)$.

C. Spectral Regrowth

The autocorrelation of the third-order response is

$$\begin{aligned} &E\Big\{y_3(0)y_3(\tau)\Big\} \\ &= a_3^2\overline{V_c^6}E\Big\{i^3i_\tau^3+q^3q_\tau^3+3i^3i_\tau q_\tau^2+3i^2qq_\tau^3 \\ &\qquad +3ii_\tau^3q^2+3i_\tau^2q^3q_\tau+9i^2i_\tau^2qq_\tau+9ii_\tau q^2q_\tau^2\Big\} \end{aligned}$$

where the products with an odd number of the $i(t)$ or $q(t)$ components of $c(t)$ were omitted because their averages are zero. Lengthy derivations give the following PSD of in-band $y_3(t)$:

$$S_{\text{SR}}(\Omega) = \begin{cases} \dfrac{3a_3^2\overline{V_c^6}}{32B}\left[3\Omega^2(\Omega^2+1)+22\right], & |\Omega| \le 1 \\ \dfrac{3a_3^2\overline{V_c^6}}{128B}(3-|\Omega|)^2(3\Omega^2-8|\Omega|+9), & 1 < |\Omega| \le 3. \end{cases}$$

Converting $S_{\text{SR}}(\Omega)$ into the power within Δf gives

$$P_{\text{SR}}(\Omega) \approx \begin{cases} \dfrac{P_o^3\Delta f\left[3\Omega^2(\Omega^2+1)+22\right]}{12\cdot OIP_3^2B}, & |\Omega| \le 1 \\ \dfrac{P_o^3\Delta f(3-|\Omega|)^2(3\Omega^2-8|\Omega|+9)}{48\cdot OIP_3^2B}, & 1 < |\Omega| \le 3. \end{cases}$$

The $P_{\text{lin}}(\Omega)$, $P_{\text{ICD}}(\Omega)$, and $P_{\text{SR}}(\Omega)$ components of the in-band output spectrum are plotted in Fig. 3 for $P_o = -3.9$ dBm, $OIP_3 = +12.2$ dBm, and $\Delta f = 30$ kHz. The following two interesting observations can be made from their graphs.

1) $P_{\text{ICD}}(\Omega)$ dips in the middle of the channel, suggesting that the composite response exhibits a stronger gain compression/expansion closer to the channel edges. A similar spectral component for the Gaussian noise excitation is flat within the channel.
2) $P_{\text{SR}}(\Omega)$ jumps by 8.45 dB at the channel edges with the frequency moving toward the channel center. However, measurements using a feedforward cancellation technique described in [14] showed that not all of the in-channel portion of the spectral regrowth is uncorrelated to the linear response. By subtracting the fedforward CDMA excitation from the amplifier linearly-attenuated output, it was found that the uncorrelated in-channel portion of the composite response is in fact slightly below the spectral regrowth just outside the channel edges. This portion acts as an interference to other users transmitting at the same frequency. Its power spectrum is given by the following formula and shown in Fig. 3 as the in-channel portion of the total uncorrelated response (solid line):

$$P_{\text{IC, uncorr}}(\Omega) \approx \frac{P_o^3}{OIP_3^2}\frac{\Delta f}{2B}\left(\frac{\Omega^4}{2}-\frac{5\Omega^2}{6}+\frac{5}{9}\right) \quad (6)$$

for $|\Omega| \le 1$ where "IC" in the subscript stands for "in-channel."

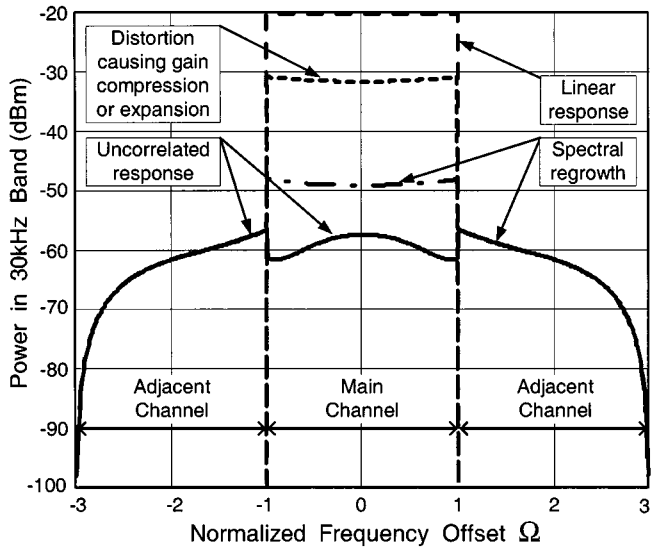

Fig. 3. In-band output spectrum components.

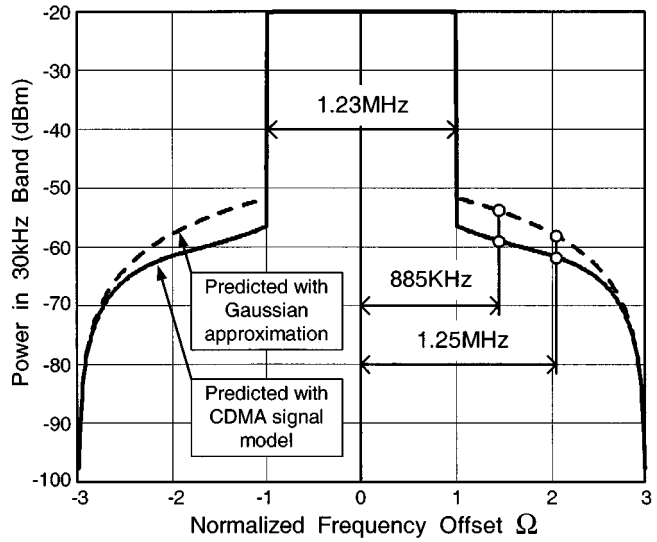

Fig. 4. Output spectra predicted with CDMA signal model and Gaussian approximation.

The power of the combined response is

$$P_{\rm comb}(\Omega) = P_{\rm lin}(\Omega) + P_{\rm ICD}(\Omega) + P_{\rm SR}(\Omega).$$

$P_{\rm comb}(\Omega)$ predicted with the CDMA signal model and Gaussian approximation is plotted in Fig. 4 for the same P_o and OIP_3. The Gaussian approximation estimates 5.1 dB more spectral regrowth at the frequency offset $f_o = 885$ kHz and 3.7 dB more at $f_o = 1.25$ MHz than the proposed CDMA signal model (1).

Several important remarks on the use of the derived formulas have to be made as follows.

1) Even though the above analysis was based on a power series, expressing a_3 in terms of OIP_3 in the final formulas for the output power components allowed to take into account the same circuit memory that affects the two-tone IMD. A Volterra series analysis in combination with statistical methods would have been extremely laborious and yet resulted in the same formulas under the assumption that the circuit transfer function is constant (but not necessarily the same) over $(f_o - B/2,\ f_o/2 + B/4)$, $(f_c - 3B/2,\ f_c + 3B/2)$, and $(2f_c - B,\ 2f_c + B)$ frequency ranges where f_o is the frequency offset from the center of a CDMA channel at which ACPR is measured.
2) The asymmetry in the spectral regrowth due to the circuit reactances in the baseband predicted by the Volterra series analysis can also be taken into account in the formula for $P_{\rm SR}(\Omega)$ by substituting $OIP_3 = OIP_{3L}$ for $\Omega < 0$ and $OIP_3 = OIP_{3R}$ for $\Omega > 0$ where OIP_{3L} and OIP_{3R} are the intercept points calculated for the left- and right-side IMD products, respectively.
3) The frequency spacing between the two tones used to simulate or measure IMD should be in the range $(f_o - B/2,\ f_o/2 + B/4)$ which is the range of the delta frequencies in the CDMA signal contributing to the spectral regrowth at the frequency offset f_o.
4) The above formulas are all applicable to both OQPSK and QPSK modulated signals.

VI. Waveform Quality Factor

Waveform quality factor ρ is a fraction of energy of the actual CDMA signal within the channel that correlates with the ideal reference signal. ρ is measured when only the pilot channel is transmitted. If the transmitted signal matches the reference perfectly, $\rho = 1$, i.e., 100% of the signal is useful information to the receiver. If $\rho < 1$, the uncorrelated signal power appears as an added noise interfering with other users in the same cell and reducing its capacity. IS-95 [20] sets the minimum ρ at 0.944 for mobile transmitters i.e., the total transmitted in-channel power should at least contain 94.4% of the correlated power. ρ is reduced by the transmitter impairments such as PN-code time offset, magnitude, phase and frequency errors in the IQ modulator, the carrier phase noise and feedthrough, the in-channel thermal noise and the third-order distortion [13]. Here only the distortion effect will be considered.

Since the linear response of the circuit $y_1(t)$ is the scaled ideal waveform, ρ can be computed as the *power correlation coefficient* (defined as the squared correlation coefficient) between $y_1(t)$ and the in-channel portion of the combined response $y(t)$. With the subscript "IC" denoting the in-channel response,

$$\rho = \frac{E\Big\{y_1(0)y_{\rm IC}(0)\Big\}^2}{E\Big\{y_1^2(0)\Big\}E\Big\{y_{\rm IC}^2(0)\Big\}}$$

where $E\{y_1(0)y_{\rm IC}(0)\}^2/E\{y_1^2(0)\}$ is the power of the correlated signal in $y(t)$ and $E\{y_{\rm IC}^2(0)\}$ is the total in-channel power. Substituting $y_{\rm IC}(0) = y_1(0) + y_{3\rm IC}(0)$, we get

$$\rho = \frac{\Big[E\Big\{y_1^2(0)\Big\} + E\Big\{y_1(0)y_{3\rm IC}(0)\Big\}\Big]^2}{E\Big\{y_1^2(0)\Big\}\Big[E\{y_1^2(0) + 2E\Big\{y_1(0)y_{3\rm IC}(0)\Big\} + E\Big\{y_{3\rm IC}^2(0)\Big\}\Big]}.$$

It can be shown that $E\{y_1(0)y_{3\rm IC}(0)\} = E\{y_1(0)y_3(0)\} = R_{y_1y_3}(0)$. $E\{y_{3\rm IC}^2(0)\}$ is the total in-channel power of $y_3(t)$ and

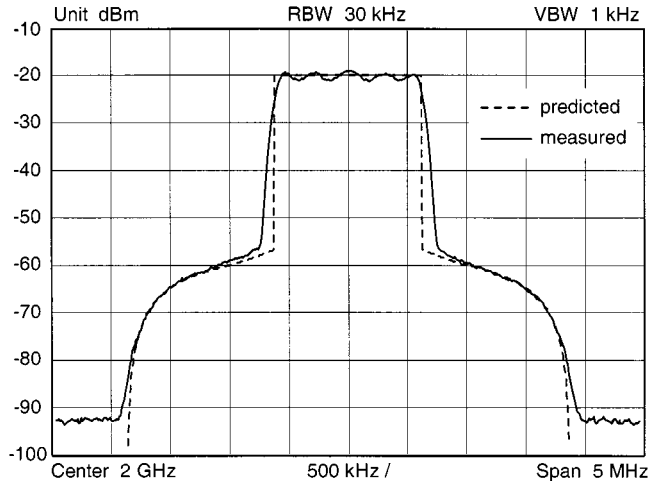

Fig. 5. Measured and predicted output spectra of the amplifier.

can be found by integrating $S_{\rm SR}(\Omega)$ within the channel ($|\Omega| \leq 1$). Thus,

$$\rho = \frac{\left[1 - 4P_o/(3 \cdot OIP_3)\right]^2}{1 - 8P_o/(3 \cdot OIP_3) + 59P_o^2/(30 \cdot OIP_3^2)}.$$

According to the above analysis, $y_3(t)$ contains a term with the power $2E\{y_1(0)y_3(0)\} = \pm 8P_o^2/(3 \cdot OIP_3)$ correlated to the linear response and causing either gain compression ($-$) or expansion ($+$) depending on the sign of a_3. The other term of $y_3(t)$ is also correlated to $y_1(t)$ and causes the gain expansion regardless of the a_3 sign. This term has the power $E\{y_1(0)y_3(0)\}^2/E\{y_1^2(0)\} = 16P_o^3/(9 \cdot OIP_3^2)$. The remaining in-channel portion of $y_3(t)$ has the power $17P_o^3/(90 \cdot OIP_3^2)$ and acts as the added noise. This is the same portion that is given by (6) and plotted in Fig. 3 as the in-channel portion of the total uncorrelated response.

VII. Measured Results

Fig. 5 shows the measured and predicted output spectra of an amplifier driven by a CDMA signal with the OQPSK modulation. The total in-channel output power is -4.0 dBm. The corresponding linear power P_o extrapolated from the small-signal measurements is -3.9 dBm. The measured OIP_3 is $+12.2$ dBm. The predicted spectrum closely follows the measured one at most frequencies. The disagreement at the channel edges is due to a nonideal rolloff of the IS-95 baseband filter response at the cut-off frequency.

Fig. 6 shows the dependence of the output power in the channel and at 1.25 MHz offset on the input power. Fig. 7 shows the waveform quality factor as a function of the input power. All powers are measured in the 30-kHz band. The disagreement between the measured and predicted results at higher input levels is explained by a stronger distortion contribution of the fifth and higher odd-order nonlinearities of the amplifier that have been neglected in the analysis. The deviation of the measured ρ from the predicted one at low input levels is caused by the clock jitter, the SAW filter generated inter-symbol interference and other impairments of the test setup.

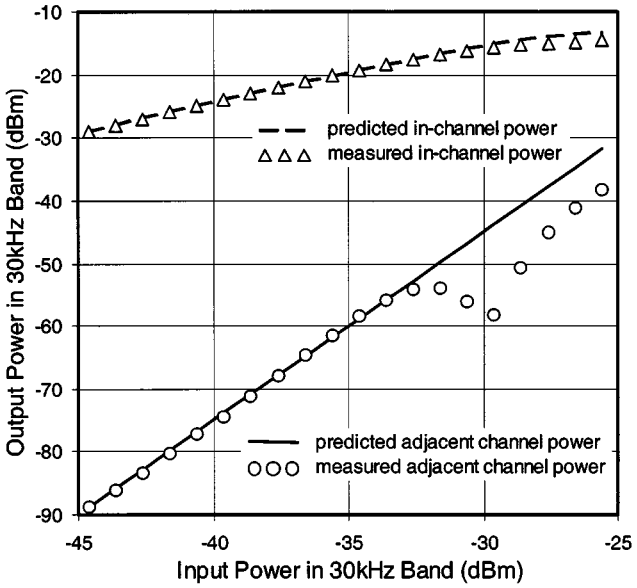

Fig. 6. In-channel and adjacent channel powers versus input power.

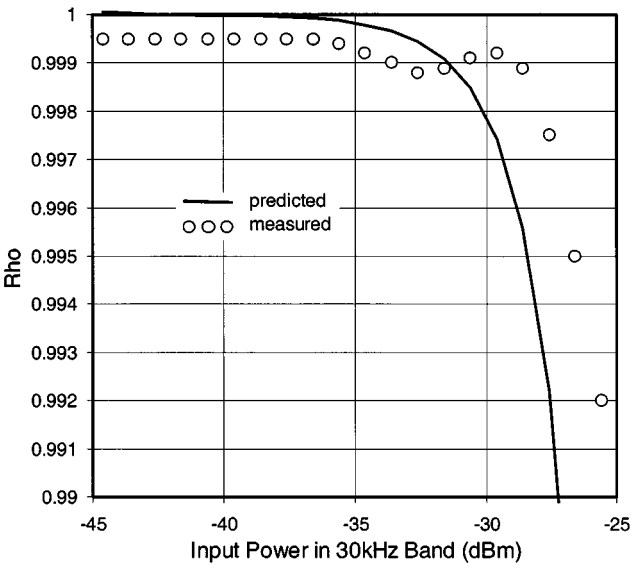

Fig. 7. Waveform quality factor ρ versus input power.

VIII. Conclusion

Using the time-domain model of the reverse-link CDMA signal, its PDF and other statistical properties are shown to be different from those of a narrow-band Gaussian noise. This difference makes the NBGN model unsuitable for analyzing the distortion in IS-95 mobile transmitters. The proposed time-domain model gives more accurate distortion estimates. The derived closed-form expressions for the spectral regrowth and waveform quality factor are valid for reverse-link and single-channel forward-link CDMA signals and include the effect of the circuit out-of-band impedances by expressing the third-order nonlinearity in terms of OIP_3. These formulas can be used in system design and analysis, but their application is limited to the cases where the third-order nonlinearity is dominant. It is possible to extend the theory toward fifth-order nonlinearity by using the shown derivations of the CDMA

signal joint moments and achieve a closer agreement between the estimated and measured distortion at higher power levels.

APPENDIX A

In this section, the autocorrelation function of the reverse-link CDMA signal $c(t)$ and NBGN $n(t)$ is derived.

For both signals, the autocorrelation of $i(t)$ is

$$\begin{aligned} R_i(\tau) &= E\Big\{ i(0)i(\tau) \Big\} \\ &= E_\theta\Big\{ \cos(\theta)\cos(\omega_c\tau+\theta) \Big\} \\ &\quad \cdot E_\phi\left\{ \sum_{k=-\infty}^{\infty}\sum_{l=-\infty}^{\infty} E\{i_k i_l\}\mathrm{sinc}(\phi/\pi-k) \right. \\ &\quad \left. \cdot\ \mathrm{sinc}(B\tau+\phi/\pi-l) \right\} \end{aligned}$$

where $E_\theta\{\,\}$ and $E_\phi\{\,\}$ are the averages over θ and ϕ, respectively. Since i_k and i_l are uncorrelated for $k \neq l$, only the summation terms with $k = l$ will be nonzero and weighted by $E\{i_k^2\} = 1$. Using the following identity [15]:

$$\sum_{k=-\infty}^{\infty} \mathrm{sinc}(\phi/\pi-k)\mathrm{sinc}(B\tau+\phi/\pi-k) = \mathrm{sinc}(B\tau)$$

we get

$$R_i(\tau) = 1/2\cos(\omega_c\tau)\mathrm{sinc}(B\tau).$$

Similarly, for $q(t)$, we obtain

$$R_q(\tau) = 1/2\cos(\omega_c\tau)\mathrm{sinc}(B\tau).$$

The cross correlation between $i(t)$ and $q(t)$ is zero because their samples are not correlated. Thus, the autocorrelation function of $c(t)$ and $n(t)$ is

$$\begin{aligned} R_c(\tau) &= R_n(\tau) = E\Big\{ \Big[i(0)+q(0) \Big]\Big[i(\tau)+q(\tau) \Big] \Big\} \\ &= R_i(\tau) + R_q(\tau) = \cos(\omega_c\tau)\mathrm{sinc}(B\tau). \end{aligned}$$

APPENDIX B

In this section, the characteristic function of the CDMA signal $c(t)$ is derived. By definition [16], this function is

$$\begin{aligned} M(v) &= E\Big\{ e^{jvc(t)} \Big\} \\ &= E\Big\{ e^{jvi(t)}e^{jvq(t)} \Big\} \\ &= \frac{1}{2\pi^2}\int_0^{2\pi} d\theta \int_0^{\pi} d\phi E_i\Big\{ e^{jvi(t)} \Big\} E_q\Big\{ e^{jvq(t)} \Big\} \end{aligned}$$

where $E_i\{\,\}$ and $E_q\{\,\}$ are the statistical averages over i_k and q_k samples, respectively. Setting t equal to 0, we get

$$\begin{aligned} &E_i\Big\{ e^{jvi(0)} \Big\} \\ &\quad = E_i\left\{ \exp\left[jv\cos(\theta)\sum_{k=-\infty}^{\infty} i_k\,\mathrm{sinc}(\phi/\pi-k) \right] \right\} \\ &\quad = \prod_{k=-\infty}^{\infty} E_i\Big\{ \exp\Big[jv\cos(\theta) i_k\,\mathrm{sinc}(\phi/\pi-k) \Big] \Big\} \\ &\quad = \prod_{k=-\infty}^{\infty} \left\{ \frac{1}{2}\exp\Big[jv\cos(\theta)(-1)\mathrm{sinc}(\phi/\pi-k) \Big] \right. \\ &\qquad \left. + \frac{1}{2}\exp\Big[jv\cos(\theta)(+1)\mathrm{sinc}(\phi/\pi-k) \Big] \right\} \\ &\quad = \prod_{k=-\infty}^{\infty} \cos\Big[v\cos(\theta)\mathrm{sinc}(\phi/\pi-k) \Big]. \end{aligned}$$

Similarly,

$$E_q\Big\{ e^{jvq(0)} \Big\} = \prod_{k=-\infty}^{\infty} \cos\Big[v\sin(\theta)\mathrm{sinc}(\phi/\pi-k+1/2) \Big].$$

Thus, the characteristic function of the CDMA signal is

$$\begin{aligned} M(v) = \frac{1}{2\pi^2}\int_0^{2\pi} d\theta \int_0^{\pi} d\phi \prod_{k=-\infty}^{\infty} &\cos\left[v\cos(\theta)\frac{\sin(\phi)}{\phi-k\pi} \right] \\ &\cdot \cos\left[v\sin(\theta)\frac{\cos(\phi)}{\phi-k\pi+\pi/2} \right] \end{aligned}$$

where the sinc function was replaced by its definition and simplified.

REFERENCES

[1] J. F. Sevic, M. B. Steer, and A. M. Pavio, "Nonlinear analysis methods for digital wireless communication systems," *Int. J. Microwave Millimeter-Wave Computer-Aided Eng.*, vol. 6, no. 3, pp. 197–216, 1996.

[2] V. Rizzoli, *et al.*, "Nonlinear processing of digitally modulated carriers by the inexact-Newton harmonic-balance technique," *Electron. Lett.*, vol. 33, no. 21, pp. 1760–1761, 1997.

[3] S. A. Maas, "Volterra analysis of spectral regrowth," *IEEE Microwave Guided Wave Lett.*, vol. 7, pp. 192–193, July 1997.

[4] D. Sharrit, "New method of analysis of communication systems," presented at the IEEE MTT-S WMFA: Nonlinear CAD Workshop, June 1996.

[5] E. Ngoya and R. Larcheveque, "Envelop transient analysis: A new method for the transient and steady state analysis of microwave communication circuits and systems," in *IEEE MTT-S Int. Microwave Symp. Dig.*, vol. 3, 1996, pp. 1365–1368.

[6] S.-W. Chen, W. Panton, and R. Gilmore, "Effect of nonlinear distortion on CDMA communication systems," *IEEE Trans. Microwave Theory Tech.*, vol. 44, pp. 2743–2750, Dec. 1996.

[7] K. Gard, H. Gutierrez, and M. Steer, "Characterization of spectral regrowth in microwave amplifiers based on the nonlinear transformation of a complex Gaussian process," *IEEE Trans. Microwave Theory Tech.*, vol. 47, pp. 1059–1069, July 1999.

[8] G. T. Zhou, "Analysis of spectral regrowth of weakly nonlinear power amplifiers," *IEEE Commun. Lett.*, vol. 4, pp. 357–359, Nov. 2000.

[9] V. Aparin and C. Persico, "Effect of out-of-band terminations on intermodulation distortion in common-emitter circuits," in *IEEE MTT-S Int. Microwave Symp. Dig.*, vol. 3, June 1999, pp. 977–980.

[10] Q. Wu, M. Testa, and R. Larkin, "On design of linear RF power amplifier for CDMA signals," *Int. J. RF Microwave Computer-Aided Eng.*, vol. 8, no. 3, pp. 283–292, 1998.
[11] N. B. Carvalho and J. C. Pedro, "Multi-tone intermodulation distortion performance of third order microwave circuits," in *IEEE MTT-S Int. Microwave Symp. Dig.*, vol. 2, June 1999, pp. 763–766.
[12] B. Buxton, S. Stanton, and J. Wolf, "ACP measurements on amplifiers designed for digital cellular and PCS systems," in *6th Annu. Wireless Symp. Dig.*, Feb. 1998, pp. 122–127.
[13] "Understanding CDMA measurements for base stations and their components," Agilent Technol., Palo Alto, CA, Applicat. Note 1311.
[14] V. Aparin, B. Butler, and P. Draxler, "Cross modulation distortion in CDMA receivers," in *IEEE MTT-S Int. Microwave Symp. Dig.*, vol. 3, 2000, pp. 1953–1956.
[15] A. Papoulis, *Signal Analysis*. New York: McGraw-Hill, 1977.
[16] W. B. Davenport and W. L. Root, *An Introduction to the Theory of Random Signals and Noise*. New York: McGraw-Hill, 1958.
[17] D. Borwein and J. M. Borwein, "Some remarkable properties of sinc and related integrals," *The Ramanujan J.*, to be published.
[18] D. E. Reed and M. A. Wickert, "Spread spectrum signals with low probability of chip rate detection," *IEEE J. Select. Areas Commun.*, vol. 7, pp. 595–601, May 1989.
[19] ——, "Nonstationary moments of a random binary pulse train," *IEEE Trans. Inform. Theory*, vol. 35, pp. 700–703, Mar. 1989.
[20] *TIA/EIA/IS-95 Mobile Station–Base Station Compatibility Standard for Dual-Mode Wideband Spectrum Cellular Systems*, July 1993.

Vladimir Aparin received the Diploma of Engineer-Physicist degree (with honors) in electronics and automatics from the Moscow Institute of Electronic Engineering (MIEE), Moscow, U.S.S.R., in 1989.

From 1987 to 1992, he was involved in the design and testing of high-speed analog and digital GaAs integrated ciruits, in the device modeling and characterization at MIEE. From 1992 to 1996, he was with Hittite Microwave Corporation, Woburn, MA, designing GaAs and Si BiCMOS RFICs for communication systems. Since 1996, he has been with QUALCOMM Inc., SanDiego, CA, designing RFIC products for CDMA systems. He is the co-author of four U.S. patents, one U.S.S.R. patent, and several technical papers.